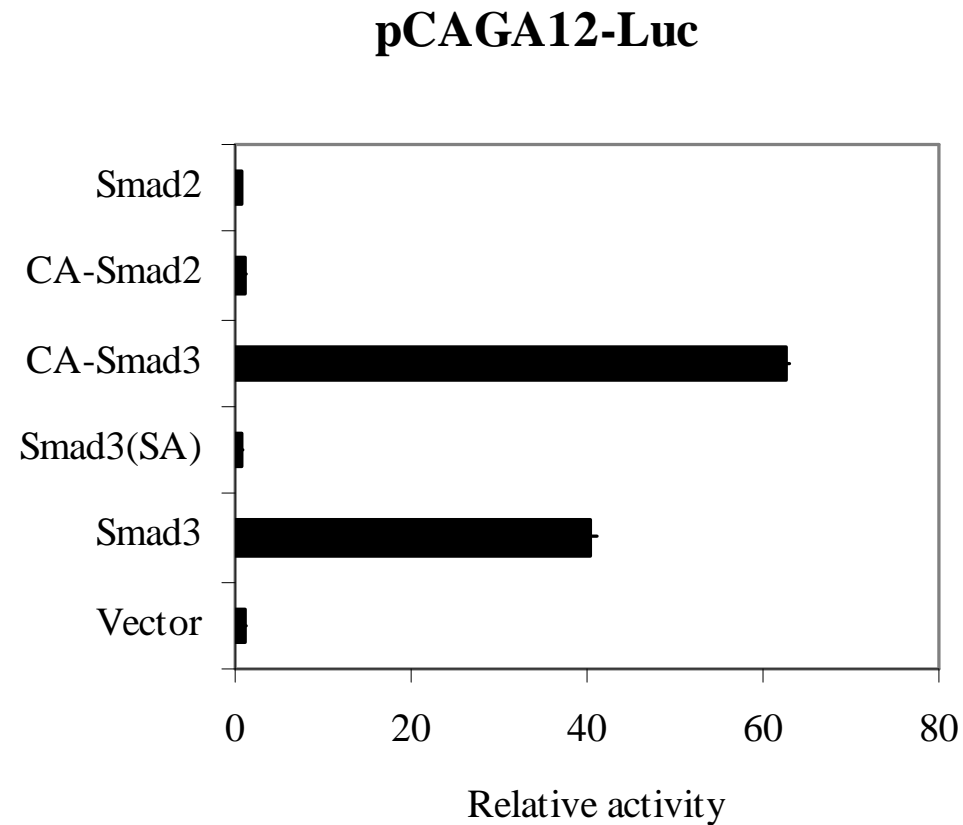
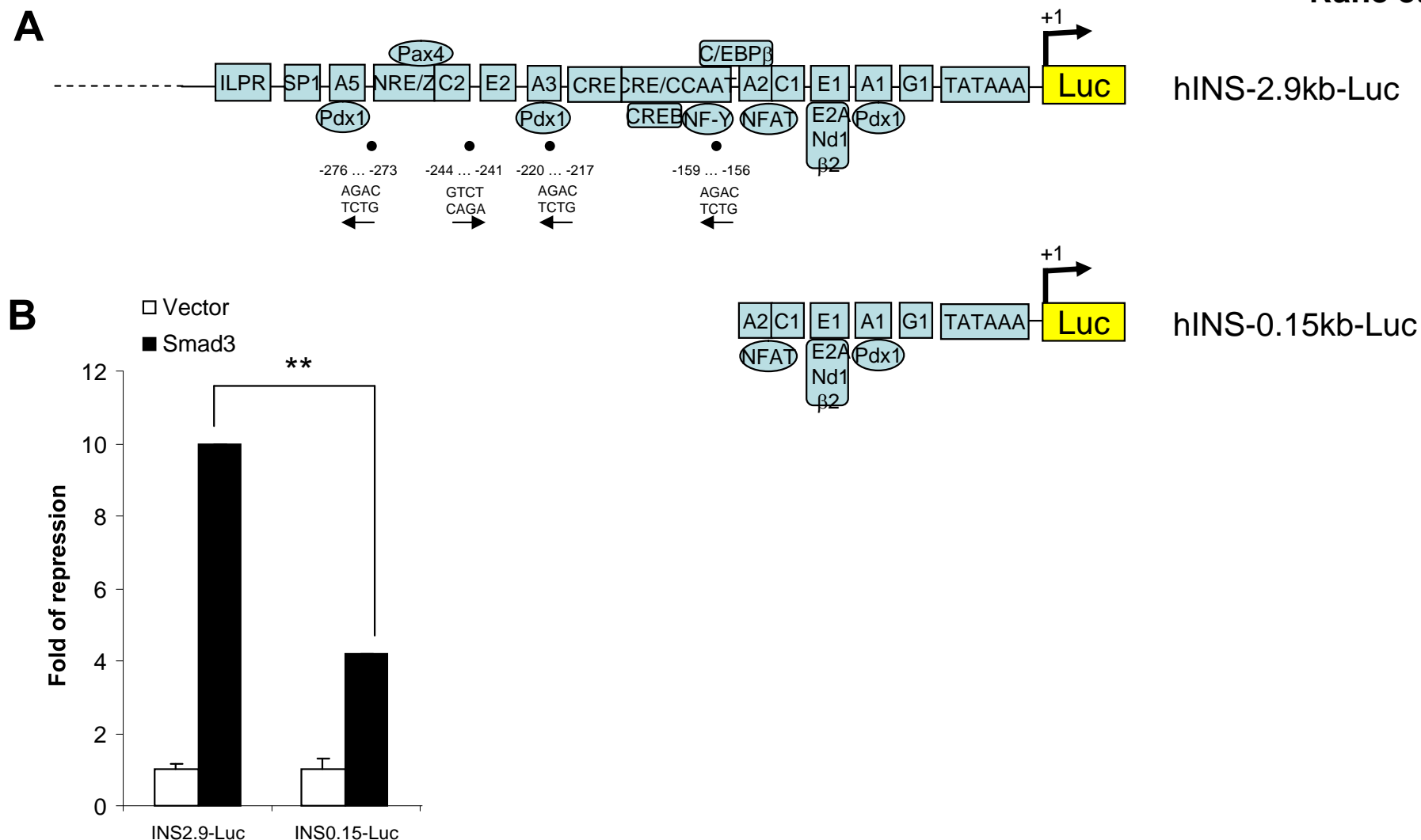


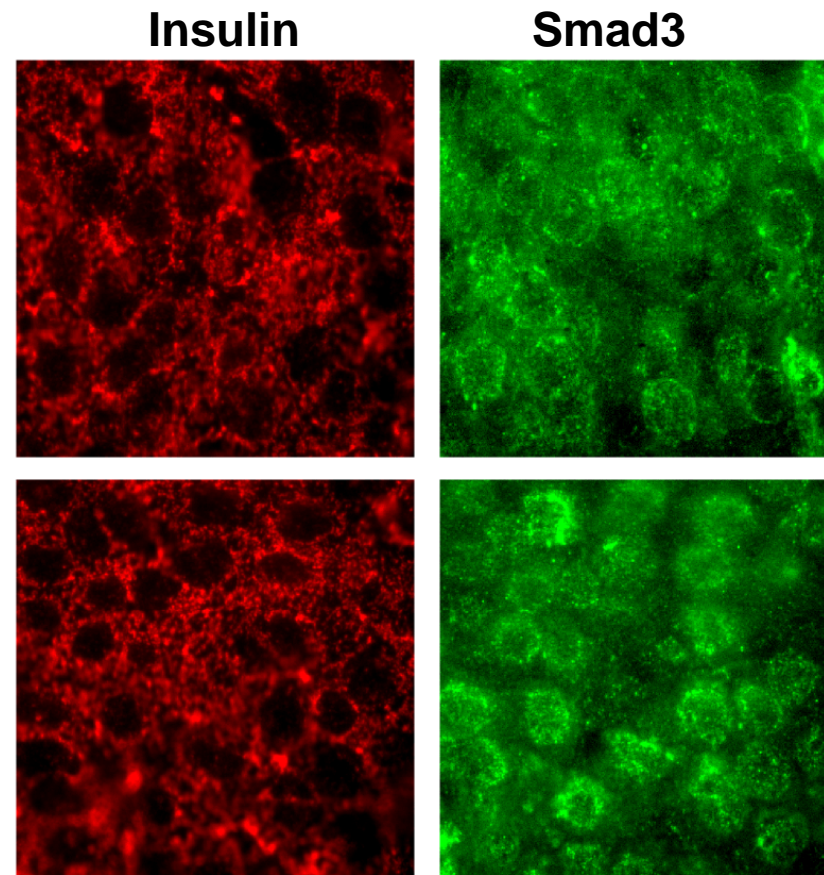
**Supplementary Figure 1.** Transduction of primary islets isolated from human cadaver donors with control adenoviruses Ad-GFP. GFP fluorescence was detected by microscopy at Day 4 after transduction of Ad-GFP in media (**A**) without serum or (**B**) containing 10% serum. Image in panel A was taken at high magnification compared to image shown in panel B. The panels on the left show phase contrast pictures while the panels on the right show GFP fluorescence.



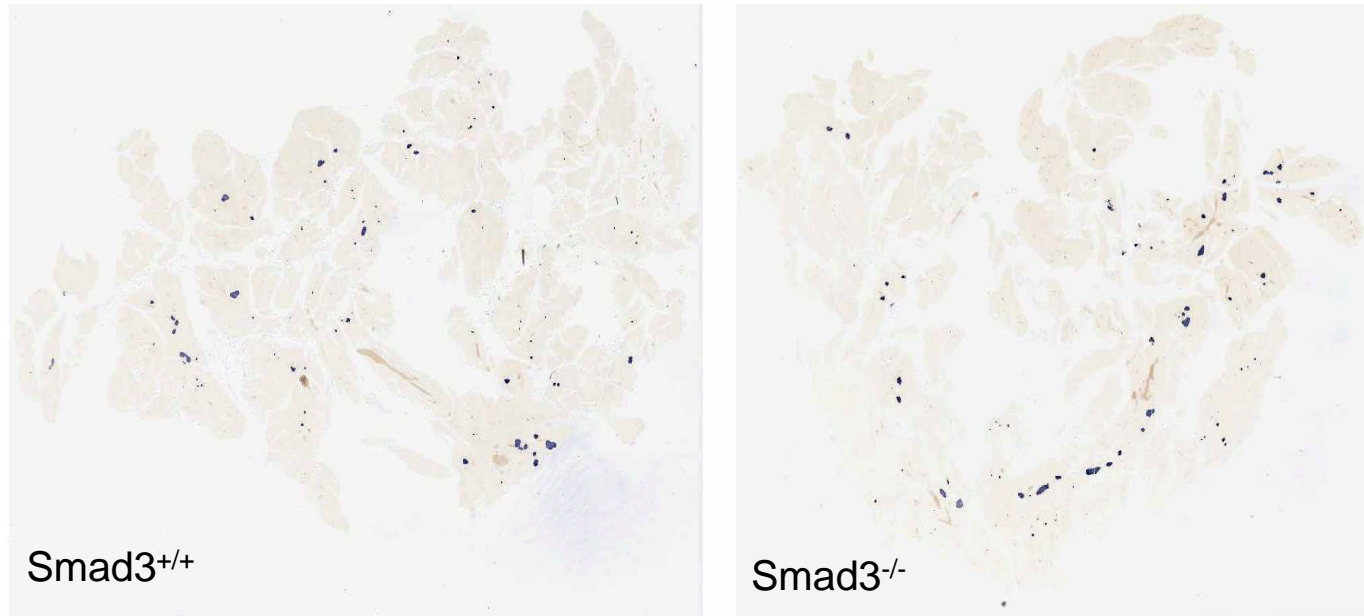
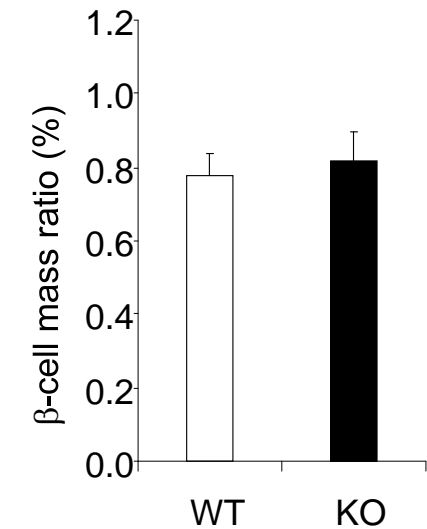
**Supplementary Figure 2.** Smad3, but not Smad2, dependent activation of CAGA12-luc reporter in INS-1E cells. Wild-type Smad3 and constitutively active Smad3 (CA-Smad3) can activate the CAGA12-luc reporter. In contrast, wild-type Smad2, CA-Smad2 or a phosphorylation-defective mutant of Smad3 (SA), cannot activate the CAGA12-luc reporter.



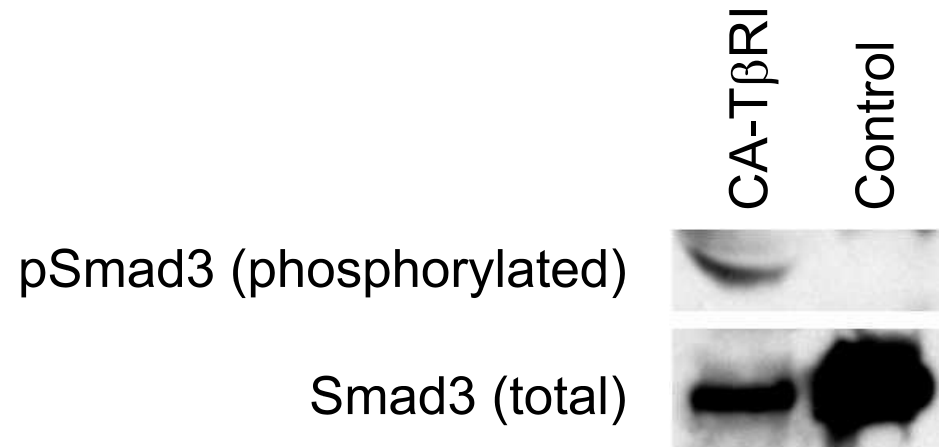
**Supplementary Figure 3. (A)** Cartoon depicting the human insulin promoter driven luciferase constructs. The hINS-2.9kb-Luc construct comprises the full length promoter. The elements representing binding sites for the key transcription factors are shown. Position and core sequences for the putative Smad3-binding sites within the first 300bp of the promoter relative to the transcription start site (+1) are identified (●). Arrows designate right or left orientation of the GTCT core elements within the putative Smad3-binding sites. The truncated hINS-0.15kb-Luc construct lacks all the putative Smad3-sites. **(B)** Relative fold repression of hINS-2.9kb-Luc and hINS-0.15kb-Luc by Smad3. INS-1E cells were transfected with luciferase constructs along with either control vector (open boxes) or Smad3 expression vectors (closed boxes) and activity of the promoter was determined. Smad3-mediated fold repression is significantly reduced in hINS-0.15kb-Luc (\*\*,  $p < 0.01$ ).



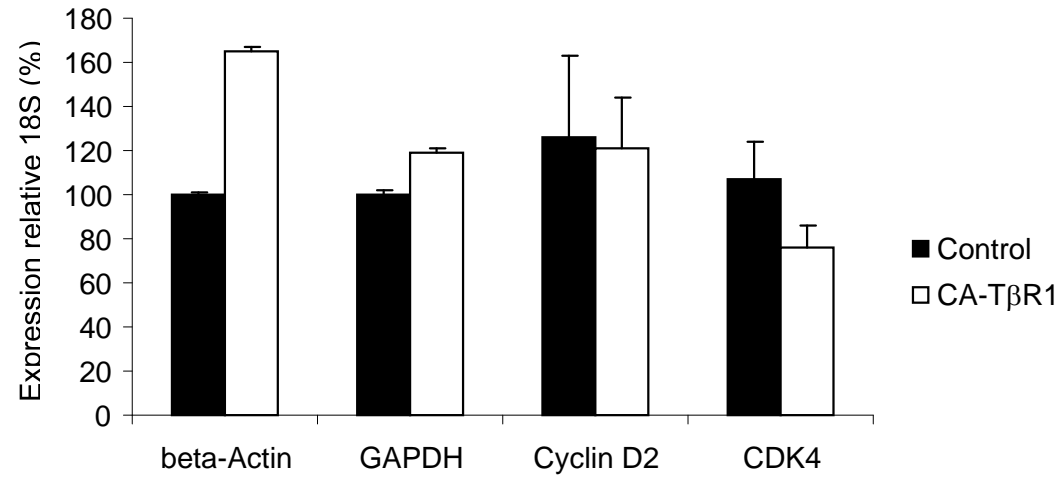
**Supplementary Figure 4.** Expression of Smad3 in islet  $\beta$ -cells. Insulin immunofluorescence was used to detect  $\beta$ -cells in pancreatic islets of *Smad3*<sup>+/+</sup> mice. Smad3 expression was detected using anti-Smad3 antibodies. Majority of insulin-expressing  $\beta$ -cells exhibit either perinuclear (top panels) or predominantly nuclear (bottom panels) Smad3.

**A****B**

**Supplementary Figure 5. (A)** Comparable pancreatic morphology as detected by insulin immunohistochemistry (purple) in two-month old *Smad3<sup>-/-</sup>* and *Smad3<sup>+/+</sup>* mice. A representative total pancreatic section is shown at a low magnification where the multilobular exocrine pancreas are light-colored and the endocrine pancreatic  $\beta$ -cells are purple-colored subsequent to insulin immunohistochemistry. **(B)**  $\beta$ -cell mass ratio, as measured by insulin immunohistochemistry (see methods for details), is similar in two-month old male *Smad3<sup>-/-</sup>* (KO; n=7) and *Smad3<sup>+/+</sup>* (WT; n=9) mice.



**Supplementary Figure 6.** INS-1E cells were untreated (control) or infected with CA-T $\beta$ RI retrovirus expressing the constitutively active (CA) form of T $\beta$ RI. Cells were harvested and extracted protein was subjected to western blot analysis using total-Smad3 antibody and anti-phospho-Smad3 antibody to detect total and phosphorylated Smad3, respectively.



**Supplementary Figure 7.** Quantitative real-time RT-PCR expression analyses of the indicated genes was performed using cDNA prepared from INS-1E cells either uninfected (closed bars) or infected with CA-TβR1 retrovirus (open bars). PCR was conducted on three independent samples and in triplicates.